

QED calculation of the ground-state energy of berylliumlike ions

A. V. Malyshev¹, A. V. Volotka^{1,2}, D. A. Glazov^{1,2,3},
I. I. Tupitsyn¹, V. M. Shabaev¹, and G. Plunien²

¹ *Department of Physics,
St. Petersburg State University,
Ulianovskaya 1, Petrodvorets,
198504 St. Petersburg, Russia*

² *Institut für Theoretische Physik,
Technische Universität Dresden,
Mommensenstraße 13, D-01062 Dresden, Germany*

³ *State Scientific Centre “Institute for Theoretical and Experimental
Physics” of National Research Centre “Kurchatov Institute”,*

*B. Cheremushkinskaya st. 25,
117218 Moscow, Russia*

Abstract

Ab initio QED calculations of the ground-state binding energies of berylliumlike ions are performed for the wide range of the nuclear charge number: $Z = 18 - 96$. The calculations are carried out in the framework of the extended Furry picture starting with three different types of the screening potential. The rigorous QED calculations up to the second order of the perturbation theory are combined with the third- and higher-order electron-correlation contributions obtained within the Breit approximation by the use of the large-scale configuration-interaction Dirac-Fock-Sturm method. The effects of nuclear recoil and nuclear polarization are taken into account. The ionization potentials are obtained by subtracting the binding energies of the corresponding lithiumlike ions. In comparison with the previous calculations the accuracy of the binding energies and the ionization potentials is significantly improved.

I. INTRODUCTION

High precision measurements of the binding energies in highly charged ions [1–12] have stimulated systematic QED calculations of these systems to all orders in the nuclear strength parameter αZ , where α is the fine structure constant and Z is the nuclear charge number. To date, such calculations up to the second-order QED contributions have been performed for H-like ions [13–15], He-like ions [16–18], Li-like ions [19–21], and B-like ions [22, 23]. In other systems the QED effects were treated using either some one-electron approximations or semiempirical methods [24–28].

The main goal of the present paper is to evaluate the ground-state energies of highly charged Be-like ions including the QED corrections up to the second order in α and the electron-correlation effects to all orders in $1/Z$. The ground-state energies of Be-like ions are of great importance for mass spectrometry [29, 30] and, along with investigations of H-, He-, Li-, and B-like ions, may also serve for tests of QED at strong fields.

Calculations of the ground-state energies and ionization potentials of berylliumlike ions have been considered by a number of authors. The full-core plus correlation method was employed for the evaluation of the ionization energies for ions with $Z \leq 25$ in Ref. [31]. This method uses the nonrelativistic multiconfiguration approach and treats the effects of relativity as the first-order perturbation. In Ref. [32] the large-scale relativistic configuration-interaction method with the Kohn-Sham screening potential was applied to calculate the energy levels of the ground and first excited states in ions with $Z = 10 - 92$. In Ref. [33] the binding energies were calculated in the Dirac-Fock approximation for different isoelectronic series. Both binding energies and ionization potentials for ions with $Z \leq 60$ were evaluated in Ref. [34] using the combination of the configuration interaction method and the many-body perturbation theory. In Ref. [35] the multiconfiguration Dirac-Fock method was employed and the ionization potentials for ions with $Z = 37 - 82$ were considered. The configuration-interaction calculation of the energy levels of berylliumlike iron ($Z = 26$) has been performed recently in Ref. [36]. All these works somehow included the radiative and nuclear recoil corrections. As a rule, only the first-order QED effects were incorporated. The necessity of a more rigorous QED treatment to improve the theoretical accuracy has been pointed out [36].

In this paper we perform *ab initio* QED calculations of the ground-state binding energies of Be-like ions in the first two orders of the perturbation theory. The perturbative QED results are merged with the third- and higher-order electron-correlation effects evaluated using the large-scale configuration-interaction Dirac-Fock-Sturm method. The calculations are carried out for the

nuclear charge number in the range: $18 \leq Z \leq 96$. In addition, we obtain the ionization potentials for Be-like ions by subtracting the binding energies of the corresponding lithiumlike ions.

The paper is organized as follows. In Sec. II we describe our approach for calculating the binding energies. In Sec. III the numerical results for the binding energies and ionization potentials are presented.

The relativistic units ($\hbar = c = 1$) and the Heaviside charge unit ($\alpha = e^2/4\pi, e < 0$) are used throughout the paper.

II. METHOD OF CALCULATION

The standard way to describe highly charged ions in the framework of QED is to use the Furry picture. To the zeroth order, this picture neglects the interaction between electrons and treats them as moving in the Coulomb field of the nucleus. Therefore, in the zeroth-order approximation the electrons obey the Dirac equation:

$$[-i\boldsymbol{\alpha} \cdot \nabla + \beta m + V_{\text{nuc}}(\mathbf{r})] \psi_n(\mathbf{r}) = \varepsilon_n \psi_n(\mathbf{r}). \quad (1)$$

The interaction between electrons and the coupling with the quantized electromagnetic field are accounted for by perturbation theory. To formulate the QED perturbation theory we use the two-time Green function (TTGF) method [37].

The convergence of the perturbation series can be accelerated by using the extended Furry picture, that is obtained by replacement of the nucleus potential V_{nuc} in Eq. (1) with the effective potential:

$$V_{\text{nuc}}(\mathbf{r}) \rightarrow V_{\text{eff}}(\mathbf{r}) = V_{\text{nuc}}(\mathbf{r}) + V_{\text{scr}}(\mathbf{r}). \quad (2)$$

The screening part $V_{\text{scr}}(\mathbf{r})$ in Eq. (2) partly accounts for the interelectronic interaction in the zeroth-order Hamiltonian. In order to avoid the double counting the counterterm $-V_{\text{scr}}$ must be added to the Feynman diagram technique. Therefore, the perturbation series are constructed in powers of the difference between the full QED interaction Hamiltonian and the screening potential. This approach is especially useful for low- Z ions, where the interelectronic interaction becomes comparable with binding energies of all electrons involved. The extended Furry picture was successfully applied to QED calculations of the energy levels [20–23, 26, 28, 38, 39], the g -factor [40], and the hyperfine splitting [41–46]. Another advantage of using the extended Furry picture, which simplifies the calculations, is avoiding the quasidegeneracy of the states $1s^2 2s^2$ and $1s^2 (2p_{1/2})^2$, that takes place for the Coulomb field.

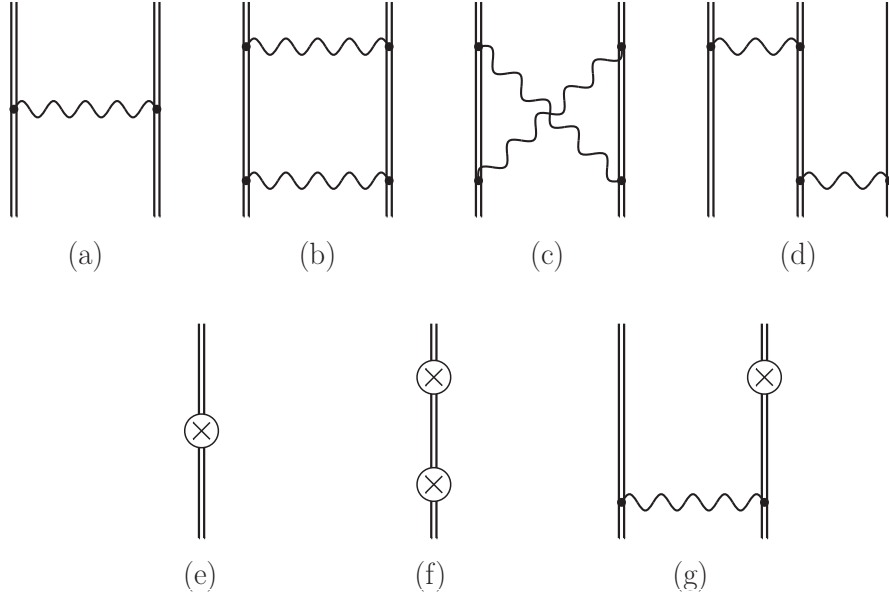


FIG. 1. The interelectronic-interaction diagrams. The double line denotes the electron moving in the effective potential (2). The symbol \otimes represents the local screening potential counterterm.

In the present work we use three different screening potentials. The first choice is the local Dirac-Fock (LDF) potential which is constructed from the wave function of the $1s^2 2s^2$ state obtained within the Dirac-Fock approximation. The derivation of the V_{LDF} potential is described in details in Ref. [47]. Two other potentials are derived within the density-functional theory. The Kohn-Sham screening potential can be written in a simple form, if one introduces the total radial charge density of all electrons:

$$\rho_t(r) = 2 \sum_{i=1s,2s} [G_i^2(r) + F_i^2(r)] , \quad (3)$$

$$\int_0^\infty \rho_t(r) dr = N, \quad (4)$$

where G/r and F/r are large and small radial components of the Dirac wave functions, and $N = 4$ is the total number of the electrons. The Kohn-Sham potential is expressed then as follows [48]:

$$V_{\text{KS}} = \alpha \int_0^\infty dr' \frac{1}{r_{>}} \rho_t(r') - \frac{2\alpha}{3} \frac{1}{r} \left(\frac{81}{32\pi^2} r \rho_t(r) \right)^{1/3}. \quad (5)$$

To improve the asymptotic behavior of this potential at large r we have added the Latter correction [49]. The third potential applied in our work is the Perdew-Zunger potential V_{PZ} [50]. This potential has been widely employed in molecular and cluster calculations.

The calculation of the binding energies of berylliumlike ions can be divided into several stages.

At the first step one has to solve Eq. (1) with an effective potential. Moreover, to perform intermediate state summations that arise in the bound states QED calculations one needs to have a quasi-complete set of the Dirac equation solutions. The numerical evaluation of the one-electron wave functions was performed using the dual kinetic balance (DKB) approach [51] with the basis functions constructed from the B-splines [52].

Next, we have calculated the set of Feynman diagrams describing the remaining interelectronic interaction. These diagrams are shown in Fig. 1. The circle with a cross denotes the screening potential counterterm. In the most of previous works the consideration was restricted to the calculation of the interaction between two $1s$ -electrons (He-like ions) or the interaction of $2s$ -electron with $1s^2$ core (Li-like ions). Since in the present work we are interested in the binding energies, we have to calculate the diagrams depicted in Fig. 1 for all possible electron configurations. For example, the diagram (*d*) is to be calculated for $1s^2 2s$ and $1s 2s^2$ subsets of electrons.

The formulas for calculation of the diagrams (*a*)-(*d*) can be found, e.g., in Refs. [19, 53]. A slight modification of the energy integration contour in the complex plane has to be performed to adopt them for the evaluation of the $2s^2$ interaction. The derivation of the formal expressions for the (*e*)-(*g*) graphs within the TTGF method is straightforward. One easily obtains:

$$\Delta E_e = 2 \sum_{a=1s,2s} V_{aa}, \quad (6)$$

$$\Delta E_f = 2 \sum_{a=1s,2s} \sum_{n \neq a} \frac{|V_{an}|^2}{\varepsilon_a - \varepsilon_n}, \quad (7)$$

$$\begin{aligned} \Delta E_g = & 4 \sum_{a=1s,2s} \sum_{n \neq a} \frac{I_{a\bar{a};n\bar{n}} V_{na}}{\varepsilon_a - \varepsilon_n} \Big|_{\mu_{\bar{a}} = -\mu_a} \\ & + \sum_{a=1s} \sum_{b=2s} \left\{ 2 \left[\sum_{n \neq b} \frac{I_{ba;na} V_{nb}}{\varepsilon_b - \varepsilon_n} + \sum_{n \neq a} \frac{I_{ab;nb} V_{na}}{\varepsilon_a - \varepsilon_n} \right] \right. \\ & \left. + (V_{aa} - V_{bb}) I'_{baab}(\varepsilon_b - \varepsilon_a) \right\}, \quad (8) \end{aligned}$$

where $V_{ab} = \langle a | -V_{\text{scr}} | b \rangle$, $I_{abcd}(\omega) = \langle ab | I(\omega) | cd \rangle$, $I(\omega) = e^2 \alpha^\mu \alpha^\nu D_{\mu\nu}(\omega)$, D is the photon propagator, $I'_{abcd}(\omega) = \langle ab | \frac{\partial}{\partial \omega} I(\omega) | cd \rangle$, $I_{ab;cd} = \langle ab | I(\Delta_{bd}) | cd \rangle - \langle ba | I(\Delta_{ad}) | cd \rangle$, $\Delta_{ab} = \varepsilon_a - \varepsilon_b$, and a and b denote the corresponding Dirac states.

The interelectronic-interaction contributions of the third and higher orders are also important. These contributions have been calculated within the Breit approximation. The configuration-interaction Dirac-Fock-Sturm method (CI-DFS) [54, 55] was used to solve the Dirac-Coulomb-Breit equation yielding the energy. The procedure of separation of the desired contribution $E_{\text{int,Breit}}^{(\geq 3)}$ from

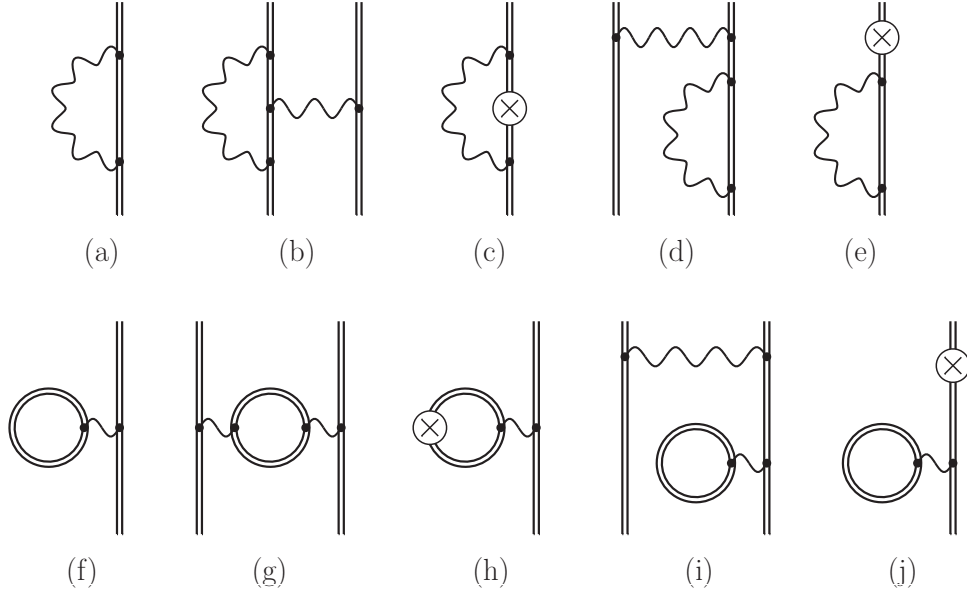


FIG. 2. First- and second-order QED diagrams (excluding the one-electron two-loop diagrams). The notations are the same as in Fig. 1.

the total result obtained in the CI-DFS calculation was described, e.g., in Refs. [20, 23]. At the intermediate stage of this procedure the first- and second-order interelectronic-interaction contributions, $E_{\text{int,Breit}}^{(1)}$ and $E_{\text{int,Breit}}^{(2)}$, have been extracted. To evaluate the accuracy of the numerical procedure we have also calculated these contributions independently using our code for the QED calculation but in the Breit approximation, i.e. calculating the (a), (b), (d)-(g) diagrams in Fig. 1 in the Coulomb gauge at the zero energy transfer and neglecting the negative-energy contribution. A very good agreement between the two different approaches was found for all three screening potentials.

At the next stage we should take into account the contributions from diagrams shown in Fig 2. In this figure, all first- and second-order QED diagrams are depicted with the exception of one-electron two-loop graphs, which will be discussed below. The diagrams in the first line are referred to as the self-energy (SE) diagrams, while in the second line the vacuum polarization (VP) diagrams are presented. Formal expressions for these diagrams derived by the TTGF method can be found, e.g., in Ref. [20]. These expressions suffer from ultraviolet divergences. The divergences in the SE diagrams are cancelled explicitly according with the renormalization scheme described in detail in Refs. [56, 57]. The VP corrections are conveniently divided into the Uehling and Wichmann-Kroll terms. In the present work the Uehling part is calculated for all VP corrections. The Wichmann-Kroll contribution of the diagrams (i)-(j) is calculated by using the approximate for-

mula for the Wichmann-Kroll potential [58]. Furthermore, this approximate potential is employed for calculation of the screening correction to the contribution of diagram (f). The one-electron Wichmann-Kroll contributions in the Coulomb field are obtained using the values presented in Ref. [59]. The Wichmann-Kroll part of the diagram (g) is relatively small [60] and has been neglected here, together with the related contribution of diagram (h).

The last second-order radiative corrections that we have to account for are given by the two-loop one-electron diagrams. The calculation of these diagrams to all orders in αZ is a very complicated task which has not yet been finished. The latest progress in this field is related to the evaluation of the two-loop self-energy diagrams. For high- Z ions the calculation of the complete set of the two-loop self-energy diagrams was performed in Ref. [61] for $n = 1, 2$ states (n is the principal quantum number). For medium- Z ions these corrections were calculated only for the $1s$ state [62, 63]. The rest of the two-loop contributions, that incorporates the diagrams with the closed fermion loop, was considered in Ref. [15] (see also Ref. [13] and references therein). The so-called *free-loop approximation* was employed there in case when the complete evaluation was not performed. In the present work, to get the two-loop corrections we interpolated the data of Refs. [15, 61–63].

Next, we have to account for the nuclear recoil corrections. The full relativistic theory of the nuclear recoil effect can be formulated only within QED. Such a theory to the first order in m/M (M is the nuclear mass) and to all orders in αZ was developed in Refs. [64, 65] (see also Refs. [66, 67] and references therein). In the Breit approximation the theory leads to the following Hamiltonian [64, 65, 68]:

$$H_M = \frac{1}{2M} \sum_{i,j} \left\{ \mathbf{p}_i \cdot \mathbf{p}_j - \frac{\alpha Z}{r_i} \left[\boldsymbol{\alpha}_i + \frac{(\boldsymbol{\alpha}_i \cdot \mathbf{r}_i) \mathbf{r}_i}{r_i^2} \right] \cdot \mathbf{p}_j \right\}. \quad (9)$$

To get the nuclear recoil correction within the Breit approximation we evaluated the expectation value of the Hamiltonian (9) with the wave functions obtained by the CI-DFS method. The nuclear recoil corrections beyond the Breit approximation, which are referred to as the QED nuclear recoil effects, have been evaluated to the zeroth order in $1/Z$. Since all the electrons in the ground state of a berylliumlike ion ($1s^2 2s^2$) have the same parity, in the zeroth order in $1/Z$ the two-electron QED recoil corrections vanish [69]. Therefore, we have to account for the one-electron QED recoil corrections only and, therefore, can use the related results for hydrogenlike ions. In Refs. [70, 71] the one-electron QED recoil corrections have been calculated for extended nuclei to all orders in αZ . Here we interpolate the data from these works.

Finally, for high- Z ions one has to take into account the effect of nuclear polarization. This correction results from the electron-nucleus interaction diagrams, in which the intermediate nuclear

TABLE I. Individual contributions to the ground-state binding energy of berylliumlike calcium (in eV).

See text for details.

Contribution	LDF	KS	PZ
$E_{\text{Dirac}}^{(0)}$	-11618.844	-11704.702	-11782.120
$E_{\text{int}}^{(1)}$	-1219.511	-1134.281	-1056.673
$E_{\text{int,Breit}}^{(2)}$	-10.996	-9.725	-11.997
$E_{\text{int,QED}}^{(2)}$	0.007	0.007	0.007
$E_{\text{int,Breit}}^{(\geq 3)}$	1.983	1.340	3.423
$E_{\text{int,total}}$	-12847.360	-12847.360	-12847.359
$E_{\text{QED}}^{(1)}$	3.366	3.419	3.383
$E_{\text{ScrQED}}^{(2)}$	0.086	0.032	0.068
$E_{\text{QED}}^{(2l)}$	-0.003	-0.003	-0.003
$E_{\text{QED,total}}$	3.449	3.448	3.448
$E_{\text{Rec,Breit}}$	0.176	0.176	0.176
$E_{\text{Rec,QED}}$	0.001	0.001	0.001
E_{total}	-12843.734	-12843.736	-12843.735

states are excited. We incorporate this correction using the results of Refs. [72–74].

To complete the discussion of the computation details it is worth noting that the numerical procedure for the evaluation of the QED corrections was checked by using two gauges, the Feynman and the Coulomb ones. Both calculations agreed very well with each other. The calculations were performed for extended nuclei using the Fermi nuclear-charge distribution with a thickness parameter of 2.3 fm. The nuclear radii were taken from Refs. [75].

III. NUMERICAL RESULTS AND DISCUSSIONS

In this section we present our results for the ground-state binding energies and ionization potentials in berylliumlike ions.

The individual contributions to the ground-state binding energies of berylliumlike calcium, xenon, and uranium calculated for the three screening potentials are collected in Tables I–III, respectively. For each ion the first line displays the binding energy $E_{\text{Dirac}}^{(0)}$ obtained as a sum of the one-electron Dirac energies. For uranium we added the nuclear deformation correction following the results of Ref. [76]. In the second line the contribution of the first-order diagrams presented in Fig. 1 is given (diagrams (a) and (e)). The diagram (a) is calculated within QED, i.e. the

TABLE II. Individual contributions to the ground-state binding energy of berylliumlike xenon (in eV).

See text for details.

Contribution	LDF	KS	PZ
$E_{\text{Dirac}}^{(0)}$	-97572.523	-97768.436	-98000.517
$E_{\text{int}}^{(1)}$	-3485.820	-3290.179	-3058.046
$E_{\text{int,Breit}}^{(2)}$	-15.206	-14.299	-16.762
$E_{\text{int,QED}}^{(2)}$	0.264	0.248	0.265
$E_{\text{int,Breit}}^{(\geq 3)}$	1.745	1.127	3.521
$E_{\text{int,total}}$	-101071.540	-101071.538	-101071.540
$E_{\text{QED}}^{(1)}$	97.763	98.240	97.904
$E_{\text{ScrQED}}^{(2)}$	0.651	0.170	0.507
$E_{\text{QED}}^{(2l)}$	-0.242	-0.242	-0.242
$E_{\text{QED,total}}$	98.173	98.168	98.169
$E_{\text{Rec,Breit}}$	0.404	0.404	0.404
$E_{\text{Rec,QED}}$	0.045	0.045	0.045
E_{total}	-100972.919	-100972.921	-100972.922

difference of the reference-state energies is kept in the photon propagator of the exchange part. In the third row we give the contribution of the second-order diagrams in Fig. 1 evaluated using the Breit approximation. We note that we consider the Coulomb and Breit photons on an equal footing. Therefore, the exchange by two Breit photons belongs to the second order term. This way to account for the Breit interaction differs from the way of Yerokhin *et al.* [39], where the Breit interaction is considered to the first order only. Moreover, in the Ref. [39] the negative energy continuum was partly accounted for in the correction under consideration. The fourth line contains the QED correction $E_{\text{int,QED}}^{(2)}$ to the third line, that is defined as the difference between the calculations of the second-order diagrams in the framework of the rigorous QED approach and the Breit approximation. In the fifth line we give the electron-correlation contribution of the third and higher orders in the Breit approximation obtained from the CI-DFS calculations. The sixth row displays the sum of all the previous terms (lines from first to fifth), $E_{\text{int,total}}$. From Tables I–III it is seen that the $E_{\text{int,total}}$ values are in a good agreement with each other for all screening potentials.

The contributions of the first- and second-order diagrams in Fig. 2 are given in the seventh and eighth rows, respectively. The ninth line contains the contribution of the two-loop one-electron diagrams. In the row labeled $E_{\text{QED,total}}$ we present the sum of the contributions of the QED diagrams (lines from seventh to ninth). Again one can see that the results of the

TABLE III. Individual contributions to the ground-state binding energy of berylliumlike uranium (in eV).

See text for details.

Contribution	LDF	KS	PZ
$E_{\text{Dirac}}^{(0)}$	-320572.56	-320871.02	-321276.02
$E_{\text{int}}^{(1)}$	-6637.37	-6338.62	-5933.84
$E_{\text{int,Breit}}^{(2)}$	-20.88	-20.45	-23.97
$E_{\text{int,QED}}^{(2)}$	2.04	1.96	2.05
$E_{\text{int,Breit}}^{(\geq 3)}$	3.03	2.39	6.05
$E_{\text{int,total}}$	-327225.74	-327225.74	-327225.74
$E_{\text{QED}}^{(1)}$	618.61	620.18	618.97
$E_{\text{ScrQED}}^{(2)}$	0.73	-0.86	0.36
$E_{\text{QED}}^{(2l)}$	-2.92	-2.92	-2.92
$E_{\text{QED,total}}$	616.41	616.40	616.41
$E_{\text{Rec,Breit}}$	0.60	0.60	0.60
$E_{\text{Rec,QED}}$	0.56	0.56	0.56
$E_{\text{Nucl.Pol.}}$	-0.45	-0.45	-0.45
E_{total}	-326608.62	-326608.63	-326608.63

calculations for all screening potentials are in a good agreement with each other. In the next two lines we give the nuclear recoil correction calculated in the Breit approximation using the CI-DFS method and the QED recoil effect evaluated to the zeroth order in $1/Z$, respectively. In Table III for berylliumlike uranium the row $E_{\text{Nucl.Pol.}}$ presents the contribution of the nuclear polarization effect. Finally, the total values of the ground-state binding energies are given in the last lines. From Tables I–III it is seen that the total values of the binding energies are almost independent of the screening potential. Hence, for all other ions we have performed the calculations using only the LDF screening potential.

The binding energy of an ion can be obtained by summing the ionization energies of all its constituent electrons. In case of a berylliumlike ion it means that one should sum the ionization potentials of the H-, He-, Li-, and Be-like ions. The corresponding compilation can be found in the NIST database [77]. In this compilation the ionization energies of hydrogenlike ions are taken from the work of Johnson and Soff [78]. The ionization potentials for heliumlike ions almost for all nuclei of interest are obtained from the paper by Artemyev *et al.* [18]. The exceptions are the He-like radium, thorium, plutonium and curium. For these ions the energies are taken from the work of Drake [79]. The ionization potentials for lithiumlike ions were calculated by Sapirstein and

TABLE IV. Ground-state binding energies (in eV) of berylliumlike ions with $Z = 18 - 96$

Nucl.	This work	Other theory	NIST	Nucl.	This work	Other theory	NIST
$^{40}_{18}\text{Ar}$	-10321.030(40)	-10321.23 ^a	-10320.73(30)	$^{132}_{54}\text{Xe}$	-100972.921(85)	-100973.7 ^a	-100963(4)
$^{40}_{20}\text{Ca}$	-12843.735(41)	-12843.96 ^a	-12843.29(40)			-100973.75 ^b	
		-12843.989 ^b		$^{138}_{56}\text{Ba}$	-109050.461(95)	-109051.1 ^a	-109039(4)
$^{48}_{22}\text{Ti}$	-15646.995(43)	-15647.31 ^a	-15646.42(50)	$^{140}_{58}\text{Ce}$	-117486.45(11)	-117486.8 ^a	-117476(5)
$^{52}_{24}\text{Cr}$	-18732.687(44)	-18733.04 ^a	-18731.96(50)	$^{142}_{60}\text{Nd}$	-126288.97(12)	-126288.9 ^a	-126279(5)
$^{56}_{26}\text{Fe}$	-22102.960(45)	-22103.37 ^a	-22102.1(1.8)	$^{152}_{62}\text{Sm}$	-135465.89(14)		-135455(6)
		-22103.299 ^b		$^{158}_{64}\text{Gd}$	-145027.69(16)	-145028.63 ^b	-145017(10)
		-22102.98(8) ^c		$^{164}_{66}\text{Dy}$	-154983.99(20)		-154974(10)
$^{58}_{28}\text{Ni}$	-25760.181(45)	-25760.64 ^a	-25759.1(2.1)	$^{166}_{68}\text{Er}$	-165345.88(21)		-165336(20)
$^{64}_{30}\text{Zn}$	-29706.959(46)	-29707.48 ^a	-29705.7(2.5)	$^{174}_{70}\text{Yb}$	-176124.31(25)		-176110(40)
$^{74}_{32}\text{Ge}$	-33946.148(47)	-33946.75 ^a	-33945(3)	$^{180}_{72}\text{Hf}$	-187332.39(28)		-187320(50)
		-33946.575 ^b		$^{184}_{74}\text{W}$	-198983.71(32)	-198984.71 ^b	-198987(3)
$^{80}_{34}\text{Se}$	-38480.835(47)	-38481.51 ^a	-38479(3)	$^{192}_{76}\text{Os}$	-211091.88(37)		-211080(70)
$^{84}_{36}\text{Kr}$	-43314.394(48)	-43315.13 ^a	-43313(4)	$^{194}_{78}\text{Pt}$	-223674.28(44)		-223660(90)
$^{88}_{38}\text{Sr}$	-48450.485(50)	-48451.27 ^a	-48449(4)	$^{202}_{80}\text{Hg}$	-236746.09(52)		-236730(100)
$^{90}_{40}\text{Zr}$	-53893.040(51)	-53893.88 ^a	-53891(5)	$^{208}_{82}\text{Pb}$	-250326.80(59)	-250327.64 ^b	-250310(100)
$^{98}_{42}\text{Mo}$	-59646.278(54)	-59647.22 ^a	-59644(5)	$^{210}_{84}\text{Po}$	-264434.5(1.2)		-264430(100)
		-59646.894 ^b		$^{220}_{86}\text{Rn}$	-279089.7(1.5)		-279070(200)
$^{102}_{44}\text{Ru}$	-65714.838(57)	-65715.84 ^a	-65712(6)	$^{226}_{88}\text{Ra}$	-294321.8(2.5)		-294310(200)
$^{106}_{46}\text{Pd}$	-72103.637(61)	-72104.68 ^a	-72100(6)	$^{232}_{90}\text{Th}$	-310152.0(1.7)	-310152.4 ^b	-310140(200)
$^{114}_{48}\text{Cd}$	-78817.939(65)	-78819.01 ^a	-78814(7)	$^{238}_{92}\text{U}$	-326608.6(1.3)	-326608.5 ^b	-326600(300)
$^{120}_{50}\text{Sn}$	-85863.480(70)	-85864.48 ^a	-85860(7)	$^{240}_{94}\text{Pu}$	-343730.0(5.5)		-343700(300)
$^{130}_{52}\text{Te}$	-93246.244(77)	-93247.17 ^a	-93236(4)	$^{244}_{96}\text{Cm}$	-361552.4(3.6)		-361500(400)

^a Gu [34].

^b Chen and Cheng [32] with the finite nuclear size correction recalculated employing the nuclear charge radii taken from Ref. [75].

^c Yerokhin *et al.* [36].

Cheng [21]. For ionization energies of berylliumlike ions with $Z \leq 50$ the NIST database uses the tabulation by Biémont *et al.* [80]. For tungsten ($Z = 74$) the energy is obtained from the paper by Kramida and Reader [81]. For all other berylliumlike ions the potentials are extracted from the work of Rodrigues *et al.* [33]. The works [80] and [81] are closely related to experiment, since the data presented there were obtained by combining the theoretical calculations with the systematic

consideration of available spectroscopic data along different isoelectronic series.

Table IV displays the ground-state binding energies of berylliumlike ions with $Z = 18 - 96$. For calcium, xenon, and uranium the averages of the values calculated using three screening potentials are shown. For other ions the results of the calculations with the LDF potential are presented. The uncertainties, which are given in the parentheses, were obtained by summing quadratically the uncertainty due to the nuclear size effect, the uncertainty of the CI-DFS calculation, and the uncertainty due to uncalculated two-loop one-electron QED contributions and uncalculated QED corrections of third and higher orders. For uranium the nuclear size uncertainty was estimated following to Ref. [76]. For other ions this uncertainty was estimated by summing quadratically two values. The first one was obtained by varying the root-mean-square radius within its error bar presented in Ref. [75]. The second one accounts for the dependence of the nuclear size correction on the model of the nuclear charge distribution. It was evaluated as the difference of the results obtained with the Fermi model and the model of homogeneously charged sphere. The uncertainty due to uncalculated QED corrections to the interelectronic interaction of third and higher orders was conservatively estimated multiplying the term $E_{\text{int,Breit}}^{(\geq 3)}$ by the double ratio of the second order QED correction to the interelectronic interaction and the corresponding contribution calculated within the Breit approximation, $E_{\text{int,QED}}^{(2)}/E_{\text{int,Breit}}^{(2)}$. The uncertainty due to uncalculated two-loop one-electron QED terms was estimated following to Ref. [15]. Finally, we have conservatively estimated the contribution of the higher-order screened QED diagrams by multiplying the second order QED term by the factor $2/Z$. For low- Z ions the total uncertainty is mainly determined by the uncertainty of the CI-DFS calculation. For high- Z ions the uncertainties due to the nuclear size effect and uncalculated one-electron two-loop corrections play a dominant role. In Table IV we compare our binding energies with the NIST database compilation and the relativistic CI calculations by Chen and Cheng [32], Gu [34], and Yerokhin *et al.* [36]. The main uncertainty to the NIST final values comes from the ionization potentials for berylliumlike ions. This is not surprising since, as it was mentioned above, all the previous calculations of Be-like ions include the QED effects either semiempirically or in some one-electron approximations. It is seen that, as a rule, our results are in a good agreement with the previous calculations but have much higher accuracies. Some discrepancy with the NIST values is observed for several first ions with $Z > 50$. The reason of this discrepancy is unclear to us.

Finally, in Table V we present the ionization potentials for berylliumlike ions. The ionization potentials are obtained by subtracting the binding energies of Li-like ions from the binding energies

TABLE V. Ionization potentials (in eV) for berylliumlike ions with $Z = 18 - 96$

Nucleus	This work	Other work	Nucleus	This work	Other work
$^{40}_{18}\text{Ar}$	-855.754(39)	-855.47(27) ^a -855.82 ^b	$^{120}_{50}\text{Sn}$	-8106.856(64)	-8103.1(7.3) ^a -8107.2 ^b
$^{40}_{20}\text{Ca}$	-1087.273(41)	-1086.85(40) ^a -1087.3 ^b -1087.311 ^c	$^{130}_{52}\text{Te}$	-8831.121(70)	-8821(4) ^d -8831.5 ^b
$^{48}_{22}\text{Ti}$	-1346.891(43)	-1346.33(47) ^a -1347.0 ^b	$^{132}_{54}\text{Xe}$	-9590.905(76)	-9581(4) ^d -9591.4 ^b
$^{52}_{24}\text{Cr}$	-1634.822(44)	-1634.11(55) ^a -1634.9 ^b	$^{138}_{56}\text{Ba}$	-10387.024(82)	-10376(4) ^d -10388 ^b
$^{56}_{26}\text{Fe}$	-1951.307(44)	-1950.4(1.8) ^a -1951.4 ^b	$^{140}_{58}\text{Ce}$	-11220.379(91)	-11210(5) ^d -11221 ^b
$^{58}_{28}\text{Ni}$	-2296.621(45)	-2295.6(2.1) ^a -2296.7 ^b	$^{142}_{60}\text{Nd}$	-12091.91(10)	-12082(5) ^d -12092 ^b
$^{64}_{30}\text{Zn}$	-2671.061(46)	-2669.9(2.5) ^a -2671.2 ^b	$^{152}_{62}\text{Sm}$	-13002.63(11)	-12992(6) ^d
$^{74}_{32}\text{Ge}$	-3074.968(46)	-3073.6(3.0) ^a -3075.1 ^b	$^{158}_{64}\text{Gd}$	-13953.70(12)	-13943(10) ^d
$^{80}_{34}\text{Se}$	-3508.689(47)	-3507.1(3.5) ^a -3508.9 ^b	$^{164}_{66}\text{Dy}$	-14946.29(14)	-14936(15) ^d
$^{84}_{36}\text{Kr}$	-3972.628(47)	-3970.8(4.0) ^a -3972.8 ^b	$^{166}_{68}\text{Er}$	-15981.70(16)	-15971(24) ^d
$^{88}_{38}\text{Sr}$	-4467.212(48)	-4465.3(4.5) ^a -4467.4 ^b	$^{174}_{70}\text{Yb}$	-17061.27(17)	-17050(40) ^d
$^{90}_{40}\text{Zr}$	-4992.900(50)	-4990.7(5.0) ^a -4993.1 ^b	$^{180}_{72}\text{Hf}$	-18186.56(20)	-18176(50) ^d
$^{98}_{42}\text{Mo}$	-5550.194(52)	-5547.8(5.5) ^a -5550.5 ^b	$^{184}_{74}\text{W}$	-19359.16(22)	-19348(50) ^d -19362.5(3.1) ^e
$^{102}_{44}\text{Ru}$	-6139.633(54)	-6136.8(5.8) ^a -6139.9 ^b	$^{192}_{76}\text{Os}$	-20580.79(25)	-20570(70) ^d
$^{106}_{46}\text{Pd}$	-6761.805(57)	-6758.8(6.3) ^a -6762.1 ^b	$^{194}_{78}\text{Pt}$	-21853.51(28)	-21843(90) ^d
$^{114}_{48}\text{Cd}$	-7417.323(60)	-7413.9(6.8) ^a -7417.7 ^b	$^{202}_{80}\text{Hg}$	-23179.15(31)	-23168(110) ^d
			$^{208}_{82}\text{Pb}$	-24560.05(34)	-24548(120) ^d
			$^{210}_{84}\text{Po}$	-25998.65(42)	-25988(150) ^d
			$^{220}_{86}\text{Rn}$	-27497.30(48)	-27486(170) ^d
			$^{226}_{88}\text{Ra}$	-29059.53(61)	-29048(200) ^d
			$^{232}_{90}\text{Th}$	-30687.89(60)	-30677(240) ^d
			$^{238}_{92}\text{U}$	-32386.00(64)	-32374(300) ^d
			$^{240}_{94}\text{Pu}$	-34158.6(1.1)	-34147(300) ^d
			$^{244}_{96}\text{Cm}$	-36009.8(1.0)	-35996(400) ^d

^a Biémont *et al.* [80]

^b Gu [34].

^c Chung *et al.* [31].

^d Rodrigues *et al.* [33] with the uncertainty prescribed by NIST.

^e Kramida and Reader [81].

of Be-like ions presented in Table IV. We do not use the NIST compilation for lithiumlike ions directly. Instead, we sum the ionization potentials for H-, He-, and Li-like ions. For heliumlike and lithiumlike ions we use the tabulations from Refs. [18] and [21], respectively. However, we have recalculated the finite nuclear size correction to the Dirac energies of the $1s$ and $2s$ states, since in those works the calculations were performed for nuclear radii that differ from ones we use here. To obtain the ionization potentials for H-like ions, we sum all the one-electron $1s$ contributions. The self-energy contributions were obtained by interpolating the values presented in Ref. [82] with the nuclear size correction according to Ref. [83]. The contributions of the vacuum polarization diagram were taken from Ref. [42]. The two-loop one-electron QED corrections were added according to the works [15, 61–63]. To incorporate the recoil corrections we used the data presented in Ref. [70]. In Table V our ionization potentials for the berylliumlike ions are compared with other theoretical predictions. As it was mentioned above, the works [80] and [81] are semiempirical. Therefore, one can consider the corresponding values and uncertainties as some experimental limits for the ionization potentials. It can be seen that our ionization energies agree with the previous calculations but have a much higher accuracy, especially for high- Z ions.

IV. SUMMARY

To summarize, the calculations of the ground-state binding energies and ionization potentials for berylliumlike ions were performed in the range: $18 \leq Z \leq 96$. Our computational procedure allows to merge the rigorous QED calculations up to the second order of the perturbation theory with the large-scale CI-DFS evaluations of the higher-order electron-correlation contributions. As the result, the most precise theoretical predictions for the ground-state binding energies and the ionization potentials in Be-like ions have been obtained.

ACKNOWLEDGEMENTS

This work was supported by RFBR (Grants No. 13-02-00630, No. 12-03-01140, No. 14-02-31316, No. 14-02-00241, and No. 14-02-31476), by SPbSU (Grants No. 11.38.269.2014, No. 11.38.261.2014, and No. 11.0.15.2010), and by DFG (Grant No. VO 1707/1-2). A.V.M. acknowledges the support from the Dynasty foundation, G-RISC, and DAAD. The work of D.A.G. was

also supported by the FAIR-Russia Research Center and by the Dynasty foundation.

- [1] J. Schweppe, A. Belkacem, L. Blumenfeld, N. Claytor, B. Feinberg, H. Gould, V. E. Kostroun, L. Levy, S. Misawa, J. R. Mowat, and M. H. Prior, *Phys. Rev. Lett.* **66**, 1434 (1991).
- [2] T. Stöhlker, P. H. Mokler, K. Beckert, F. Bosch, H. Eickhoff, B. Franzke, M. Jung, T. Kandler, O. Klepper, C. Kozhuharov, R. Moshhammer, F. Nolden, H. Reich, P. Rymuza, P. Spädtke, and M. Steck, *Phys. Rev. Lett.* **71**, 2184 (1993).
- [3] P. Beiersdorfer, A. L. Osterheld, and S. R. Elliott, *Phys. Rev. A* **58**, 1944 (1998).
- [4] P. Beiersdorfer, A. L. Osterheld, J. H. Scofield, J. R. Crespo López-Urrutia, and K. Widmann, *Phys. Rev. Lett.* **80**, 3022 (1998).
- [5] P. Bosselmann, U. Staude, D. Horn, K.-H. Scharfner, F. Folkmann, A. E. Livingston, and P. H. Mokler, *Phys. Rev. A* **59**, 1874 (1999).
- [6] T. Stöhlker, P. H. Mokler, F. Bosch, R. W. Dunford, F. Franzke, O. Klepper, C. Kozhuharov, T. Ludziejewski, F. Nolden, H. Reich, P. Rymuza, Z. Stachura, M. Steck, P. Swiat, and A. Warczak, *Phys. Rev. Lett.* **85**, 3109 (2000).
- [7] C. Brandau, C. Kozhuharov, A. Müller, W. Shi, S. Schippers, T. Bartsch, S. Böhm, C. Böhme, A. Hoffknecht, H. Knopp, N. Grün, W. Scheid, T. Steih, F. Bosch, B. Franzke, P. H. Mokler, F. Nolden, M. Steck, T. Stöhlker, and Z. Stachura, *Phys. Rev. Lett.* **91**, 073202 (2003).
- [8] I. Draganić, J. R. Crespo López-Urrutia, R. DuBois, S. Fritzsche, V. M. Shabaev, R. S. Orts, I. I. Tupitsyn, Y. Zou, and J. Ullrich, *Phys. Rev. Lett.* **91**, 183001 (2003).
- [9] A. Gumberidze, T. Stöhlker, D. Banaś, K. Beckert, P. Beller, H. F. Beyer, F. Bosch, X. Cai, S. Hagmann, C. Kozhuharov, D. Liesen, F. Nolden, X. Ma, P. H. Mokler, A. Oršić-Muthig, M. Steck, D. Sierpowski, S. Tashenov, A. Warczak, and Y. Zou, *Phys. Rev. Lett.* **92**, 203004 (2004).
- [10] A. Gumberidze, T. Stöhlker, D. Banaś, K. Beckert, P. Beller, H. F. Beyer, F. Bosch, S. Hagmann, C. Kozhuharov, D. Liesen, F. Nolden, X. Ma, P. H. Mokler, M. Steck, D. Sierpowski, and S. Tashenov, *Phys. Rev. Lett.* **94**, 223001 (2005).
- [11] P. Beiersdorfer, H. Chen, D. B. Thorn, and E. Träbert, *Phys. Rev. Lett.* **95**, 233003 (2005).
- [12] V. Mäkel, R. Klawitter, G. Brenner, J. R. Crespo López-Urrutia, and J. Ullrich, *Phys. Rev. Lett.* **107**, 143002 (2011).
- [13] P. Mohr, G. Plunien, and G. Soff, *Phys. Rep.* **293**, 227 (1998).

- [14] V. Yerokhin, P. Indelicato, and V. Shabaev, *Eur. Phys. J. D* **25**, 203 (2003).
- [15] V. A. Yerokhin, P. Indelicato, and V. M. Shabaev, *Phys. Rev. A* **77**, 062510 (2008).
- [16] H. Persson, S. Salomonson, P. Sunnergren, and I. Lindgren, *Phys. Rev. Lett.* **76**, 204 (1996).
- [17] V. Yerokhin, A. Artemyev, and V. Shabaev, *Phys. Lett. A* **234**, 361 (1997).
- [18] A. N. Artemyev, V. M. Shabaev, V. A. Yerokhin, G. Plunien, and G. Soff, *Phys. Rev. A* **71**, 062104 (2005).
- [19] V. A. Yerokhin, A. N. Artemyev, V. M. Shabaev, M. M. Sysak, O. M. Zhrebtssov, and G. Soff, *Phys. Rev. A* **64**, 032109 (2001).
- [20] Y. S. Kozhedub, A. V. Volotka, A. N. Artemyev, D. A. Glazov, G. Plunien, V. M. Shabaev, I. I. Tupitsyn, and T. Stöhlker, *Phys. Rev. A* **81**, 042513 (2010).
- [21] J. Sapirstein and K. T. Cheng, *Phys. Rev. A* **83**, 012504 (2011).
- [22] A. N. Artemyev, V. M. Shabaev, I. I. Tupitsyn, G. Plunien, and V. A. Yerokhin, *Phys. Rev. Lett.* **98**, 173004 (2007).
- [23] A. N. Artemyev, V. M. Shabaev, I. I. Tupitsyn, G. Plunien, A. Surzhykov, and S. Fritzsche, *Phys. Rev. A* **88**, 032518 (2013).
- [24] E. Lindroth and J. Hvarfner, *Phys. Rev. A* **45**, 2771 (1992).
- [25] M. S. Safronova, W. R. Johnson, and U. I. Safronova, *Phys. Rev. A* **53**, 4036 (1996).
- [26] J. Sapirstein and K. T. Cheng, *Phys. Rev. A* **66**, 042501 (2002).
- [27] P. Indelicato, E. Lindroth, and J. P. Desclaux, *Phys. Rev. Lett.* **94**, 013002 (2005).
- [28] M. H. Chen, K. T. Cheng, W. R. Johnson, and J. Sapirstein, *Phys. Rev. A* **74**, 042510 (2006).
- [29] J. Repp, C. Böhm, J. Crespo López-Urrutia, A. Dörr, S. Eliseev, S. George, M. Goncharov, Y. Novikov, C. Roux, S. Sturm, S. Ulmer, and K. Blaum, *Appl. Phys. B* **107**, 983 (2012).
- [30] E. G. Myers, *Int. J. Mass Spectrom.* **349-350**, 107 (2013).
- [31] K. T. Chung, X.-W. Zhu, and Z.-W. Wang, *Phys. Rev. A* **47**, 1740 (1993).
- [32] M. H. Chen and K. T. Cheng, *Phys. Rev. A* **55**, 166 (1997).
- [33] G. C. Rodrigues, P. Indelicato, J. P. Santos, P. Patté, and F. Parente, *At. Data Nucl. Data Tables* **86**, 117 (2004).
- [34] M. F. Gu, *At. Data Nucl. Data Tables* **89**, 267 (2005).
- [35] J. Huang, G. Jiang, and Q. Zhao, *Chin. Phys. Lett.* **23**, 69 (2006).
- [36] V. A. Yerokhin, A. Surzhykov, and S. Fritzsche, *Phys. Rev. A* **90**, 022509 (2014).
- [37] V. M. Shabaev, *Phys. Rep.* **356**, 119 (2002).

- [38] J. Sapirstein and K. T. Cheng, Phys. Rev. A **64**, 022502 (2001).
- [39] V. A. Yerokhin, A. N. Artemyev, and V. M. Shabaev, Phys. Rev. A **75**, 062501 (2007).
- [40] D. A. Glazov, A. V. Volotka, V. M. Shabaev, I. I. Tupitsyn, and G. Plunien, Phys. Lett. A **357**, 330 (2006).
- [41] J. Sapirstein and K. T. Cheng, Phys. Rev. A **63**, 032506 (2001).
- [42] J. Sapirstein and K. T. Cheng, Phys. Rev. A **67**, 022512 (2003).
- [43] J. Sapirstein and K. T. Cheng, Phys. Rev. A **74**, 042513 (2006).
- [44] N. S. Oreshkina, A. V. Volotka, D. A. Glazov, I. I. Tupitsyn, V. M. Shabaev, and G. Plunien, Opt. Spektrosk. **102**, 889 (2007), [Opt. Spectrosc. **102**, 815 (2007)].
- [45] Y. S. Kozhedub, D. A. Glazov, A. N. Artemyev, N. S. Oreshkina, V. M. Shabaev, I. I. Tupitsyn, A. V. Volotka, and G. Plunien, Phys. Rev. A **76**, 012511 (2007).
- [46] A. V. Volotka, D. A. Glazov, I. I. Tupitsyn, N. S. Oreshkina, G. Plunien, and V. M. Shabaev, Phys. Rev. A **78**, 062507 (2008).
- [47] V. M. Shabaev, I. I. Tupitsyn, K. Pachucki, G. Plunien, and V. A. Yerokhin, Phys. Rev. A **72**, 062105 (2005).
- [48] W. Kohn and L. J. Sham, Phys. Rev. **140**, A1133 (1965).
- [49] R. Latter, Phys. Rev. **99**, 510 (1955).
- [50] J. P. Perdew and A. Zunger, Phys. Rev. B **23**, 5048 (1981).
- [51] V. M. Shabaev, I. I. Tupitsyn, V. A. Yerokhin, G. Plunien, and G. Soff, Phys. Rev. Lett. **93**, 130405 (2004).
- [52] W. R. Johnson, S. A. Blundell, and J. Sapirstein, Phys. Rev. A **37**, 307 (1988).
- [53] V. M. Shabaev and I. G. Fokeeva, Phys. Rev. A **49**, 4489 (1994).
- [54] V. F. Bratzev, G. B. Deyneka, and I. I. Tupitsyn, Izv. Acad. Nauk SSSR, Ser. Fiz. **41**, 2655 (1977), [Bull. Acad. Sci. USSR: Phys. Ser. **41**, 173 (1977)].
- [55] I. I. Tupitsyn, V. M. Shabaev, J. R. Crespo López-Urrutia, I. Draganić, R. S. Orts, and J. Ullrich, Phys. Rev. A **68**, 022511 (2003).
- [56] V. A. Yerokhin, A. N. Artemyev, T. Beier, G. Plunien, V. M. Shabaev, and G. Soff, Phys. Rev. A **60**, 3522 (1999).
- [57] V. A. Yerokhin and V. M. Shabaev, Phys. Rev. A **60**, 800 (1999).
- [58] A. G. Fainshtein, N. L. Manakov, and A. A. Nekipelov, J. Phys. B **24**, 559 (1991).
- [59] J. Sapirstein and K. T. Cheng, Phys. Rev. A **68**, 042111 (2003).

- [60] A. N. Artemyev, T. Beier, G. Plunien, V. M. Shabaev, G. Soff, and V. A. Yerokhin, Phys. Rev. A **60**, 45 (1999).
- [61] V. A. Yerokhin, P. Indelicato, and V. M. Shabaev, Phys. Rev. Lett. **97**, 253004 (2006).
- [62] V. A. Yerokhin, P. Indelicato, and V. M. Shabaev, Phys. Rev. A **71**, 040101 (2005).
- [63] V. A. Yerokhin, Phys. Rev. A **80**, 040501 (2009).
- [64] V. M. Shabaev, Teor. Mat. Fiz. **63**, 394 (1985), [Theor. Math. Phys. **63**, 588 (1985)].
- [65] V. M. Shabaev, Yad. Fiz. **47**, 107 (1988), [Sov. J. Nucl. Phys. **47**, 69 (1988)].
- [66] V. M. Shabaev, Phys. Rev. A **57**, 59 (1998).
- [67] G. S. Adkins, S. Morrison, and J. Sapirstein, Phys. Rev. A **76**, 042508 (2007).
- [68] C. W. P. Palmer, J. Phys. B: At. Mol. Phys. **20**, 5987 (1987).
- [69] A. N. Artemyev, V. M. Shabaev, and V. A. Yerokhin, Phys. Rev. A **52**, 1884 (1995).
- [70] V. M. Shabaev, A. N. Artemyev, T. Beier, G. Plunien, V. A. Yerokhin, and G. Soff, Phys. Rev. A **57**, 4235 (1998).
- [71] V. M. Shabaev, A. N. Artemyev, T. Beier, G. Plunien, V. A. Yerokhin, and G. Soff, Phys. Scr. **T80**, 493 (1999).
- [72] G. Plunien and G. Soff, Phys. Rev. A **51**, 1119 (1995), Phys. Rev. A **53**, 4614 (1996).
- [73] A. V. Nefiodov, L. N. Labzowsky, G. Plunien, and G. Soff, Phys. Lett. A **222**, 227 (1996).
- [74] A. V. Volotka and G. Plunien, Phys. Rev. Lett. **113**, 023002 (2014).
- [75] I. Angeli and K. P. Marinova, At. Data Nucl. Data Tables **99**, 69 (2013).
- [76] Y. S. Kozhedub, O. V. Andreev, V. M. Shabaev, I. I. Tupitsyn, C. Brandau, C. Kozhuharov, G. Plunien, and T. Stöhlker, Phys. Rev. A **77**, 032501 (2008).
- [77] A. Kramida, Yu. Ralchenko, J. Reader, and NIST ASD Team, NIST Atomic Spectra Database (ver. 5.1), [Online]. Available: <http://physics.nist.gov/asd> [2014, July 17]. National Institute of Standards and Technology, Gaithersburg, MD. (2013).
- [78] W. R. Johnson and G. Soff, At. Data Nucl. Data Tables **33**, 405 (1985).
- [79] G. W. Drake, Can. J. Phys. **66**, 586 (1988).
- [80] E. Biémont, Y. Frémat, and P. Quinet, At. Data Nucl. Data Tables **71**, 117 (1999).
- [81] A. E. Kramida and J. Reader, At. Data Nucl. Data Tables **92**, 457 (2006).
- [82] P. J. Mohr, Phys. Rev. A **46**, 4421 (1992).
- [83] V. A. Yerokhin, Phys. Rev. A **83**, 012507 (2011).